Simple solvable model for heavy-fermion superconductivity from the two-fluid normal state

Jiangfan Wang [1,*] Yu Li,[2,3] and Yi-feng Yang [4,5,6]

[1] *School of Physics, Hangzhou Normal University, Hangzhou, Zhejiang 311121, China*
[2] *Institute of Quantum Materials and Physics, Henan Academy of Sciences, Zhengzhou, Henan 450046, China*
[3] *Kavli Institute for Theoretical Sciences, University of Chinese Academy of Sciences, Beijing 100190, China*
[4] *Beijing National Laboratory for Condensed Matter Physics and Institute of Physics, Chinese Academy of Sciences, Beijing 100190, China*
[5] *School of Physical Sciences, University of Chinese Academy of Sciences, Beijing 100190, China*
[6] *Songshan Lake Materials Laboratory, Dongguan, Guangdong 523808, China*

(Received 27 September 2023; revised 17 December 2023; accepted 9 February 2024; published 27 February 2024)

Heavy-fermion superconductors exhibit unusual properties such as low transition temperatures, large specific heat jumps, and normal states with universal two-fluid behaviors. Standard theoretical models such as the Anderson or Kondo lattices often require uncontrolled approximations to solve. Here, we propose an exactly solvable Kondo lattice model with a local-in-momentum Kondo interaction, which can be derived from an Anderson lattice with a Hatsugai-Kohmoto interaction between f electrons. As the Kondo coupling increases, the normal state evolves from a Fermi liquid to a non-Fermi liquid two-fluid state. With a pairing interaction between electrons, the model exhibits a crossover from a weak-coupling superconductor to a strong-coupling one showing many important features of heavy-fermion superconductivity, including the formation of Kondo-induced composite-fermion Cooper pairs, the analog of heavy-electron Cooper pairs in real materials.

DOI: 10.1103/PhysRevB.109.064517

I. INTRODUCTION

Heavy-fermion compounds are prototypical strongly correlated electron systems that exhibit unconventional superconductivity [1–3]. Due to strong electron correlations and interplay between multiple degrees of freedom, heavy-fermion superconductors (HFSCs) are known for their rich diversity of order parameter structures and pairing mechanisms [4–12]. Despite such a diversity, they share important macroscopic features. For example, they are often formed out of an unusual two-fluid normal state, where physical quantities are contributed by two different parts: a Kondo liquid part associated with the itinerant heavy electrons, and a classical spin liquid part associated with the residual unhybridized local spins [13–23]. The two-fluid normal state is also responsible for the coexistence of superconductivity and magnetic order observed in many heavy-fermion materials [20,24]. Other common features of HFSCs include their low transition temperatures, large jump anomaly of the specific heat, and often a large ratio between the superconducting gap and the transition temperature [2,25–30]. Therefore, seeking an efficient way to describe both the two-fluid normal state and the universal features of HFSCs emerging from it is an important issue in this area.

Previous studies of HFSCs are based on either phenomenological models with effective pairing interaction [31,32] or Anderson/Kondo lattice models that inevitably rely on analytical or numerical approximations [33–37]. Most of these studies focus on certain microscopic properties, but fail to make a connection between the superconductivity and the two-fluid normal state. The problem is rooted in the difficulty of dealing with the strong f-electron interaction, and the lack of a satisfactory microscopic theory for the two-fluid behaviors despite several earlier attempts [38–44]. Recently, it was found that the exactly solvable Hatsugai-Kohmoto (HK) model may provide a convenient tool to study strongly correlated electron systems [45–57]. The model assumes an all-to-all nonlocal interaction that transforms to a local one in momentum space, which represents a stable interacting fixed point closely relevant to the Mott physics [45–48], unconventional superconductivity [46–51], and correlated topological materials [55–57]. Inspired by this, we recently proposed a momentum-space Kondo lattice model, whose solution reveals the coexistence of Kondo and spin liquids akin to the heavy-fermion two-fluid states [58]. A microscopic definition of the Kondo liquid "order parameter" was found, which exhibits a universal scaling consistent with experiments [58]. The Schrieffer-Wolf (SW) transformation relates this **k**-space Kondo lattice to a modified Anderson lattice with HK interaction between f electrons. As we will show, these models do capture many important features of heavy-fermion materials.

In this paper, we introduce a BCS pairing interaction to the **k**-space Kondo lattice model, and study superconductivity emerged from the two-fluid normal state. By increasing the Kondo coupling, we found a crossover from a weak-coupling BCS superconductor to a strong-coupling superconductor as the corresponding normal state evolves from a Fermi liquid to a non-Fermi liquid (NFL) two-fluid state. The latter is featured with low transition temperatures and significant enhancement of both the gap ratio and the specific heat jump anomaly relative to the BCS values, consistent with the HFSC. In

[*] jfwang@hznu.edu.cn

addition, the Kondo effect leads to different types of Cooper pairs formed by composite fermions (composite objects of conduction electrons and f-spin fluctuations), which are the analog of heavy-electron Cooper pairs in real materials. Our exactly solvable model thus provides a different perspective to study the heavy-fermion superconductors and their normal states.

II. MODEL AND RESULTS

We start from the Hamiltonian containing conduction electrons, f electrons (H_f), and a general form of Kondo-like spin-flip scattering between them:

$$H = \sum_{ij}(t_{ij} - \mu\delta_{ij})c^{\dagger}_{i\alpha}c_{j\alpha} + H_f + \sum_{iji'j'} \frac{J_{iji'j'}}{4\mathcal{N}_s} c^{\dagger}_{i\alpha}\boldsymbol{\sigma}_{\alpha\beta}c_{i'\beta}\cdot f^{\dagger}_{j\gamma}\boldsymbol{\sigma}_{\gamma\delta}f_{j'\delta}\delta_{\mathbf{r}_i+\mathbf{r}_j,\mathbf{r}_{i'}+\mathbf{r}_{j'}}, \tag{1}$$

where repeated indices imply summations, and $\mathcal{N}_s$ is the number of lattice sites. The δ function keeps the center of mass of the two particles conserved in the scattering process. The translational invariance requires that the coupling constant $J_{iji'j'}$ depend only on $\mathbf{r}_i - \mathbf{r}_j$ and $\mathbf{r}_i - \mathbf{r}_{i'}$. Other than the local Kondo interaction, Eq. (1) includes nonlocal c-f scatterings that represent collective Kondo hybridizations at low temperatures in a dense Kondo lattice, which should be important for understanding the two-fluid phenomenology [21].

To make the scattering term mathematically tractable, we assume a constant coupling $J_{iji'j'} = J_K$, so that it simply becomes $\frac{J_K}{4}\sum_{\mathbf{k}} c^{\dagger}_{\mathbf{k}\alpha}\boldsymbol{\sigma}_{\alpha\beta}c_{\mathbf{k}\beta}\cdot f^{\dagger}_{\mathbf{k}\gamma}\boldsymbol{\sigma}_{\gamma\delta}f_{\mathbf{k}\delta}$. Similar infinitely ranged all-to-all interactions were studied in the Sachdev-Ye-Kitaev (SYK) model [59] and the HK model [45]. We further assume the f electrons described by H_f are in a perfect Mott insulating state such that every $\mathbf{k}$ point in the Brillouin zone is singly occupied. Then one can replace the f electrons with a well-defined spin operator $\mathbf{S}_{\mathbf{k}} = \frac{1}{2}\sum_{\gamma\delta} f^{\dagger}_{\mathbf{k}\gamma}\boldsymbol{\sigma}_{\gamma\delta}f_{\mathbf{k}\delta}$, and arrives at the $\mathbf{k}$-space Kondo lattice model:

$$H_K = \sum_{\mathbf{k}\alpha}\epsilon_{\mathbf{k}}c^{\dagger}_{\mathbf{k}\alpha}c_{\mathbf{k}\alpha} + \frac{J_K}{2}\sum_{\mathbf{k}\alpha\beta}c^{\dagger}_{\mathbf{k}\alpha}\boldsymbol{\sigma}_{\alpha\beta}c_{\mathbf{k}\beta}\cdot\mathbf{S}_{\mathbf{k}}. \tag{2}$$

Such a featureless Mott state of f electrons can indeed be obtained from the HK Hamiltonian [45–48,52,57]:

$$H_f = \sum_{\mathbf{k}}\xi_{\mathbf{k}}n^f_{\mathbf{k}} + U\sum_{\mathbf{k}}n^f_{\mathbf{k}\uparrow}n^f_{\mathbf{k}\downarrow}, \tag{3}$$

where the double occupancy in momentum space is penalized by a Hubbard-U-type repulsion. This interaction leads to a breakdown of Fermi liquid and gives rise to Mott physics. At half filling, the exact solution of H_f reveals a quantum phase transition between a NFL metal and a Mott insulator as U increases [46]. This leads to the constraint $n^f_{\mathbf{k}} = 1$ and the $\mathbf{k}$-space f spins deep inside the Mott insulating state. Therefore, one can derive Eq. (2) more rigorously by combining Eq. (3) with the usual c-f hybridization term,

$$H_c + H_{\text{hyb}} = \sum_{\mathbf{k}\alpha}\epsilon_{\mathbf{k}}c^{\dagger}_{\mathbf{k}\alpha}c_{\mathbf{k}\alpha} + \mathcal{V}\sum_{\mathbf{k}\alpha}(c^{\dagger}_{\mathbf{k}\alpha}f_{\mathbf{k}\alpha} + \text{H.c.}), \tag{4}$$

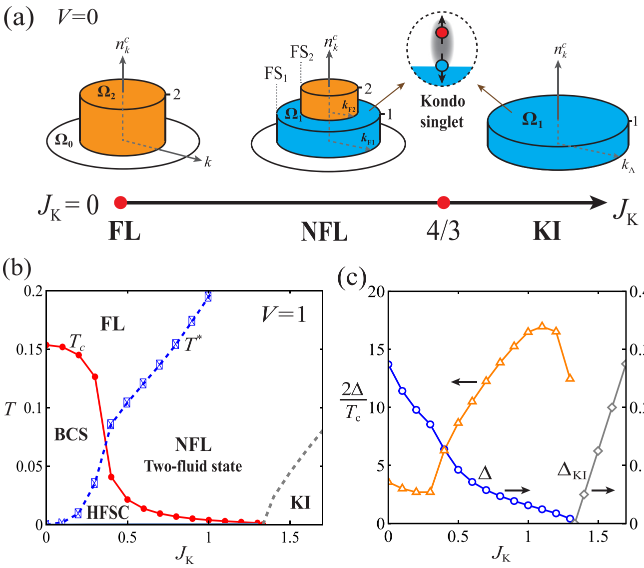

FIG. 1. (a) Three different ground states of the $\mathbf{k}$-space Kondo lattice model H_K as J_K increases: Fermi liquid (FL), non-Fermi liquid (NFL) metal, and Kondo insulator (KI). The conduction electron occupation number $n^c_{\mathbf{k}}$ is shown for each phase. Kondo singlets only reside on the singly occupied region Ω_1. (b) The phase diagram of the $\mathbf{k}$-space Kondo-BCS model with pairing interaction $V = 1$. (c) The energy gap for the superconducting state (Δ) and the KI state (Δ_{KI}), and the superconducting gap ratio $2\Delta/T_c$ at different J_K.

and performing a SW transformation of this modified Anderson lattice model. As shown in Appendix A, this gives the relation $J_K \approx 8|\mathcal{V}|^2/U$ for large U.

A. Normal states

Equation (2) can be exactly solved since the local Hilbert space at each $\mathbf{k}$ can be independently diagonalized. Figure 1(a) shows the ground-state phase diagram of H_K and the corresponding conduction electron occupation number $n^c_{\mathbf{k}}$. For simplicity, here we have assumed a parabolic dispersion $\epsilon_{\mathbf{k}} = k^2/2\pi - 1$ with an ultraviolet cutoff $k_\Lambda = 2\sqrt{\pi}$, so that the half-bandwidth $D = 1$ serves as the energy unit, and the electron density is $n_c = \mathcal{N}_s^{-1}\sum_{\mathbf{k}} n^c_{\mathbf{k}} = 1$ throughout our calculations. At $J_K = 0$, the conduction electrons form a Fermi liquid (FL) that is completely decoupled from the f spins. A finite J_K destroys the Fermi liquid by replacing the original Fermi surface with a singly occupied momentum region Ω_1, separated from the empty region (Ω_0) and the doubly occupied region (Ω_2) by two filling surfaces at momenta k_{F1} and k_{F2}, here denoted as FS_1 and FS_2. The appearance of three occupation regions with two filling surfaces is a hallmark of NFL ground states in HK-like models [45,60,61]. The exact Green's function of conduction electrons reveals quasiparticle excitations at FS_1 and FS_2, with dispersions reminiscent of the mean-field c-f hybridized dispersions in the usual Kondo lattice (see Appendix B). The f spins form $\mathbf{k}$-space Kondo singlets with conduction electrons only in the Ω_1 region, while remaining free in Ω_0 and Ω_2, since the Pauli principle forbids spin-flip scattering at a doubly occupied $\mathbf{k}$ point. As J_K increases, the Ω_1 region also enlarges, until it covers the entire momentum space at $J_K = 4/3$, beyond which the system enters into a Kondo insulating (KI) phase due to the complete screening of f spins. The above picture does not change qualitatively with the spatial dimension of the system.

The partial Kondo screening in the NFL state has two consequences: (1) The Mott insulated f electrons in Ω_1 become itinerant through the Kondo hybridization, such that the total number of charge carriers per spin is now counted by the "Fermi volume" enclosed by FS_1, which is larger than the Fermi volume at $J_K = 0$ but smaller than the standard large Fermi volume of a heavy-Fermi-liquid state. Such a partially enlarged Fermi volume is also found in previous large-N [62–64] or numerical calculations [65] for strongly frustrated or one-dimensional Kondo lattices where nonlocal Kondo interactions play an important role. (2) The itinerant Kondo singlets in Ω_1 form a Kondo liquid, with an "order parameter" satisfying a universal scaling consistent with the phenomenological two-fluid model [58]. The remaining unhybridized f spins in Ω_0 and Ω_2 form another fluid that is generally referred to as a "spin liquid." Moreover, the conduction electrons in Ω_0 and Ω_2 also form a third liquid, as implicitly assumed in the two-fluid model [21]. The above NFL properties persist within a finite temperature region below the characteristic Kondo coherence temperature T^* as shown in Fig. 1(b), above which the thermal fluctuations destroy the Kondo singlets and the normal state becomes a Fermi liquid just like the trivial fixed point at $J_K = 0$.

B. Superconductivity

To study the superconducting instability, we consider the simplest s-wave pairing interaction between conduction electrons,

$$H_V = -\frac{V}{\mathcal{N}_s}\sum_{\mathbf{k}\mathbf{k}'} c^\dagger_{\mathbf{k}\uparrow} c^\dagger_{-\mathbf{k}\downarrow} c_{-\mathbf{k}'\downarrow} c_{\mathbf{k}'\uparrow}, \tag{5}$$

and calculate the electron pair-binding energy, $E_b = \langle\psi|H'|\psi\rangle - \langle G|H'|G\rangle$, where $H' = H_K + H_V$, $|G\rangle$ is the ground state of H_K, and $|\psi\rangle$ is the state with an additional Cooper pair (see Appendix C). The resulting E_b satisfies

$$1 = \frac{V}{16D}\ln\left|\frac{(2D - E_b)^4(3J_K - E_b)}{-(3J_K/2 - E_b)^4 E_b}\right|, \tag{6}$$

and the numerical results are shown in Appendix C. At $J_K = 0$, Eq. (6) reduces to the BCS result. Increasing J_K reduces the absolute value $|E_b|$, but E_b stays negative throughout the entire NFL state for arbitrarily small V, indicating Cooper instability. Next, we choose a finite V and perform a BCS mean-field decomposition of H_V, and solve the combined Hamiltonian:

$$H = H_K + H_{\mathrm{BCS}},$$
$$H_{\mathrm{BCS}} = \Delta_c \sum_{\mathbf{k}} c^\dagger_{\mathbf{k}\uparrow} c^\dagger_{-\mathbf{k}\downarrow} + \mathrm{H.c.} + \frac{\mathcal{N}_s \Delta_c^2}{V}, \tag{7}$$

where $\Delta_c = -V\mathcal{N}_s^{-1}\sum_{\mathbf{k}}\langle c_{-\mathbf{k},\downarrow} c_{\mathbf{k}\uparrow}\rangle$ is the pairing amplitude. Equation (7) is still exactly solvable, since it can be written as $H = \frac{1}{2}\sum_{\mathbf{k}} H_{\mathbf{k}}$, where each $H_{\mathbf{k}}$ is a conserved quantity with a 64-dimensional Hilbert space, hence can be exactly diagonalized.

The phase diagram for $V = 1$ is shown in Fig. 1(b). A superconducting phase is found for $J_K < 4/3$, with the transition temperature T_c decreasing monotonically with increasing J_K. A rapid suppression of T_c is found between $J_K = 0.3$ and 0.4, where the phase boundary changes its sign of curvature. At this point, the normal state also evolves from a FL to a NFL two-fluid state. The crossover temperature T^* is determined by a broad maximum of the specific heat coefficient associated with the Kondo effect. Without pairing interaction, T^* decreases almost linearly with J_K and vanishes at $J_K = 0$. With finite pairing interaction, T^* continues to exist below T_c albeit being suppressed, which separates the superconducting phase into two regions: a weak-coupling BCS superconductor and a strong-coupling superconductor which we simply denote as HFSC because of its many similarities with heavy-fermion superconductors. The superconducting transition is continuous for $J_K \leqslant 0.5$ but becomes weakly first order for $J_K \geqslant 0.6$, where Δ_c jumps discontinuously at T_c (see Appendix D). We notice that the first-order transition is not rare in studies of superconductivity emerging from non-Fermi liquids [51,66]. The interaction-driven superconductor-to-insulator quantum phase transition at $J_K = 4/3$ is another interesting topic that may have experimental relevance [67,68], which we leave for future investigation.

Figure 1(c) plots the zero-temperature superconducting energy gap Δ and the gap ratio $2\Delta/T_c$, as well as the Kondo insulating gap Δ_{KI} at $J_K > 4/3$. Note that Δ is determined by the electron spectral function, which is generally unequal to the pairing amplitude Δ_c, except for $J_K = 0$ where the BCS relation holds. The gap ratio is quite close to (less than) the universal BCS value 3.53 for $J_K \leqslant 0.3$, but becomes significantly enhanced for $J_K \geqslant 0.4$, with a maximal value $2\Delta/T_c \approx 17$ at $J_K = 1.1$. Such an extremely large gap ratio is also found in quantum critical models where the pairing glue has a power-law local susceptibility [69,70], or superconductivity emerged from incoherent metals with SYK interactions [66]. In our case, we attribute the large gap ratio at $J_K \geqslant 0.4$ to the unusual Kondo liquid in the normal state, which suppresses T_c and induces another type of Cooper pair that is strongly coupled in nature.

To distinguish the two regions of the superconducting state, we define a composite fermion operator $F_{\mathbf{k}\alpha}$, and study its pairing correlation:

$$\Delta_F(\mathbf{k}) = -\langle F_{-\mathbf{k}\downarrow} F_{\mathbf{k}\uparrow}\rangle, \quad F_{\mathbf{k}\alpha} = \sum_\beta \boldsymbol{\sigma}_{\alpha\beta}\cdot\mathbf{S}_{\mathbf{k}} c_{\mathbf{k}\beta}. \tag{8}$$

In heavy-fermion literature, the composite fermion is usually defined in the coordinate space, which transforms to a convolution in the momentum space [71–73]. For the $\mathbf{k}$-space Kondo model studied here, Eq. (8) is a more appropriate definition, since the SW transformation used to derive H_K also transforms the f-electron operator $f_{\mathbf{k}\alpha}$ to $F_{\mathbf{k}\alpha}$ (see Appendix E). Therefore, one can view $F_{\mathbf{k}\alpha}$ as the renormalized f electrons in the Kondo lattice model. A finite $\Delta_F(\mathbf{k})$ indicates the presence of composite fermion Cooper pairs, which requires both pairing interaction and Kondo entanglement.

Figure 2(a) compares the temperature evolution of $\Delta_c(\mathbf{k}) = -\langle c_{-\mathbf{k}\downarrow} c_{\mathbf{k}\uparrow}\rangle$, $\Delta_F(\mathbf{k})$, and the entropy distribution $s(\mathbf{k}) = -\frac{1}{2}\mathrm{Tr}[\rho_{\mathbf{k}}\ln\rho_{\mathbf{k}}]$ ($\rho_{\mathbf{k}}$ is the density matrix of $H_{\mathbf{k}}$) for $J_K = 0.1$. Above $T_c \approx 0.152$, both $\Delta_c(\mathbf{k})$ and $\Delta_F(\mathbf{k})$ are zero, while $s(\mathbf{k})$ shows a peak around the bare ($J_K = 0$)

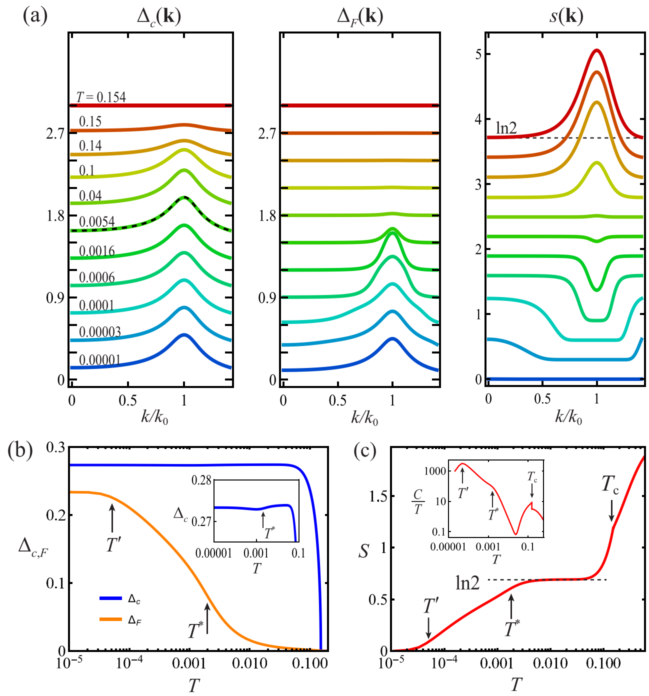

FIG. 2. (a) Evolution of $\Delta_c(\mathbf{k})$, $\Delta_F(\mathbf{k})$, and $s(\mathbf{k})$ with decreasing temperature at $J_K = 0.1$. For clarity, the data curves are shifted with each other by a constant 0.3. The black dashed line in $\Delta_c(\mathbf{k})$ is the BCS result, $\Delta_c(\mathbf{k}) = \Delta_c/(2\sqrt{\epsilon_{\mathbf{k}}^2 + \Delta_c^2})$. (b) The pairing amplitudes Δ_c and Δ_F as functions of temperature at $J_K = 0.1$. The inset shows a zoom-in view of Δ_c. (c) The entropy as a function of temperature at $J_K = 0.1$. The inset shows the specific heat coefficient.

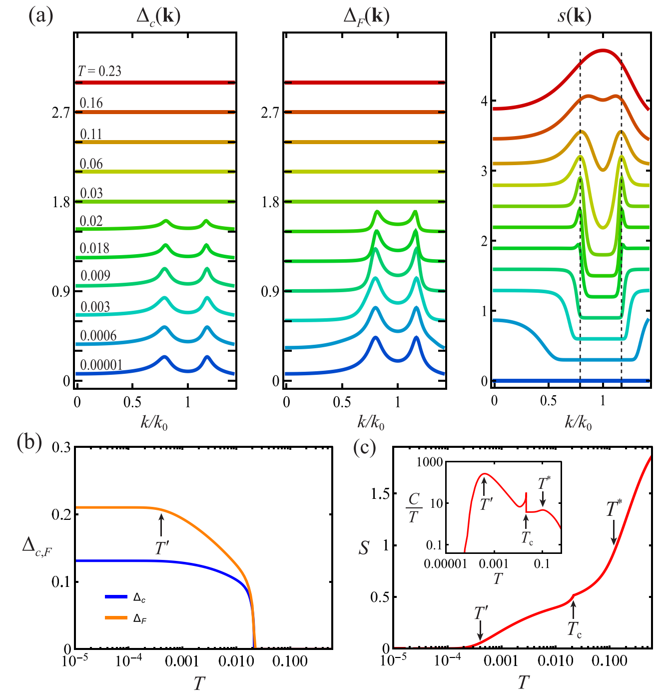

FIG. 3. (a) Temperature evolution of $\Delta_c(\mathbf{k})$, $\Delta_F(\mathbf{k})$, and $s(\mathbf{k})$ for $J_K = 0.5$. The data curves are shifted with each other by a constant 0.3. The dashed lines in $s(\mathbf{k})$ mark the positions of the two filling surfaces at $k_{F1} = 1.17k_0$ and $k_{F2} = 0.79k_0$. (b) The pairing amplitudes Δ_c and Δ_F as functions of temperature at $J_K = 0.5$. (c) The entropy as a function of temperature at $J_K = 0.5$. The inset shows the specific heat coefficient.

Fermi momentum $k_0 = \sqrt{2\pi}$, with a constant background $\ln 2$ contributed by the free f spins. Below T_c, $\Delta_c(\mathbf{k})$ becomes finite for all values of $\mathbf{k}$, while $\Delta_F(\mathbf{k})$ is almost zero within a broad range of temperature. The shape of $\Delta_c(\mathbf{k})$ can be fitted perfectly by the BCS formula $\Delta_c(\mathbf{k}) = \Delta_c/(2\sqrt{\epsilon_{\mathbf{k}}^2 + \Delta_c^2})$ as shown in Fig. 2(a). The entropy peak around k_0 is gradually consumed by the conduction electrons forming Cooper pairs, leaving a constant $\ln 2$ plateau of local spins, which is also clearly seen in the integrated entropy $S = \mathcal{N}_s^{-1}\sum_{\mathbf{k}} s(\mathbf{k})$ as shown in Fig. 2(c). Below the characteristic temperature $T^* \approx 0.002$, a large number of f spins start to combine with conduction electrons to form composite fermion Cooper pairs, as indicated by the peak of $\Delta_F(\mathbf{k})$ and the dip of $s(\mathbf{k})$ around k_0. Interestingly, the rapid development of composite pairs is accompanied by a slight suppression of the conduction electron pair amplitude, as shown by the temperature dependence of $\Delta_c = V\mathcal{N}_s^{-1}\sum_{\mathbf{k}} \Delta_c(\mathbf{k})$ and $\Delta_F = V\mathcal{N}_s^{-1}\sum_{\mathbf{k}} \Delta_F(\mathbf{k})$ in Fig. 2(b). This suggests that some Cooper pairs unbind themselves in order to form the composite pairs, indicating that these are indeed different types of Cooper pairs.

Just below T^*, the peak of $\Delta_F(\mathbf{k})$ is concentrated in the vicinity of k_0, which quickly extends to the entire momentum space as the system approaches zero temperature. The same happens to the dip (gap) of $s(\mathbf{k})$, indicating all the f spins finally become a part of the superconducting condensate. This process happens within a small temperature window, but consumes the extensive f-spin entropy in the Ω_0 and Ω_2 regions, giving rise to a huge peak of C/T at another characteristic temperature T'. Due to this huge peak, the broad maximum of C/T at T^* now appears as a shoulder, as shown in the inset of Fig. 2(c). Below T', Δ_F saturates to a constant, while S approaches zero. This characteristic temperature exists for all $0 < J_K < 4/3$; see for example Fig. 3 for $J_K = 0.5$. However it may not occur in real materials, since a more natural way to consume the extensive spin entropy is to form a nearby or coexisting magnetic order as observed in many HFSCs.

Figure 3 shows the same physical quantities at $J_K = 0.5$. Above $T_c \approx 0.021$, both $\Delta_c(\mathbf{k})$ and $\Delta_F(\mathbf{k})$ are zero, while $s(\mathbf{k})$ evolves from a single peak to two peaks centered around the two filling surfaces at $k_{F1} = 1.17k_0$ and $k_{F2} = 0.79k_0$. The entropy depletion between k_{F1} and k_{F2} is due to the formation of Kondo singlets in the Ω_1 region. It causes a broad maximum of C/T at $T^* \approx 0.1$, as shown in the inset of Fig. 3(c). Superconductivity occurs at $T_c \approx 0.021$, above which the Kondo singlets in the Ω_1 region have already been fully developed. Therefore, both the conduction electrons and composite fermions form Cooper pairs immediately below T_c. The two-peak structure of $\Delta_c(\mathbf{k})$ and $\Delta_F(\mathbf{k})$ suggests that the Cooper pairs are mainly formed by quasiparticles around the two filling surfaces, similar to the HK model [46,51]. Below T_c, the pairing amplitudes Δ_c and Δ_F increase monotonically with decreasing temperature as shown in Fig. 3(b). Different from the case of $J_K = 0.1$, here Δ_F is much larger than Δ_c, indicating that the composite fermion Cooper pairs play a dominant role.

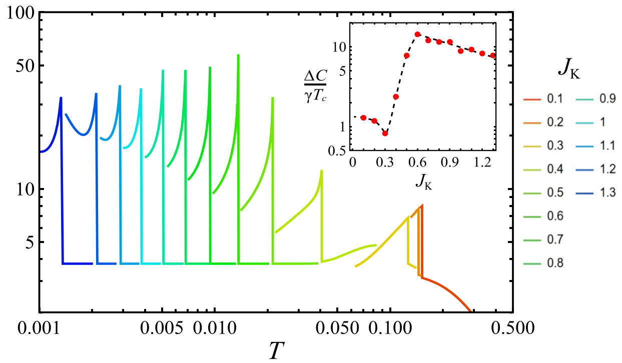

FIG. 4. The specific heat coefficient around the superconducting transition temperature at different J_K. Inset: The specific heat anomaly $\Delta C/\gamma T_c$ as a function of J_K.

Since the superconducting transitions for $J_K \geqslant 0.4$ require f spins around the two filling surfaces to form composite Cooper pairs, they consume more entropy and lead to large specific heat anomaly $\Delta C/\gamma T_c$, as shown in Fig. 4. Here, the Sommerfeld coefficient $\gamma = 3.77$ is universal for the two-fluid normal state within $0 < J_K < 4/3$, which is only slightly larger than the noninteracting value $\gamma = \pi^2/3 \approx 3.29$ at $J_K = 0$. It may require local-in-space Kondo interaction to obtain a γ as large as in real heavy-fermion materials. As J_K increases, $\Delta C/\gamma T_c$ first decreases for $J_K \leqslant 0.3$, then increases rapidly for $0.4 \leqslant J_K \leqslant 0.6$, and decreases again for $J_K \geqslant 0.6$ where the superconducting transition becomes first order. For continuous transitions within $0 < J_K < 0.6$, the evolution of $\Delta C/\gamma T_c$ follows that of the gap ratio, indicating the same microscopic origin behind them. For a rough comparison, experiments on two of the most studied strong-coupling HFSCs, $CeCoIn_5$ and $CeRhIn_5$, show $\Delta C/\gamma T_c = 4.5 \sim 4.7$ [5,74], $2\Delta/T_c = 6 \sim 10$ [26,75], and $\Delta C/\gamma T_c = 4.2$ [27], $2\Delta/T_c = 5$ [76], consistent with our results at $J_K = 0.4 \sim 0.5$.

III. DISCUSSION AND CONCLUSION

We have checked different values of V and the results remain qualitatively the same. Our method can be conveniently generalized to d-wave or p-wave pairing interactions. In all cases, the combined effect of Kondo and electron pairing interaction leads to the formation of composite-fermion Cooper pairs, corresponding to the heavy-electron Cooper pairs in real materials. An implication of our study is that the light conduction electron pairs and "heavy" composite fermion pairs may coexist in heavy-fermion superconductors reflecting the two-fluid nature of their normal states. A similar conclusion has been drawn from earlier studies [77]. What remains unexplored in this work is the microscopic mechanism behind the pairing interaction, which is often associated with the f-spin fluctuations in real materials. It is found that a Heisenberg exchange interaction between $\boldsymbol{S}_{\mathbf{k}}$ and $\boldsymbol{S}_{-\mathbf{k}}$ indeed induces pairing correlation between conduction electrons, which may require additional scattering to establish phase coherence [58].

Our method can be generalized to the multiband Kondo lattice, where each unit cell contains one f impurity and M conduction electron sites. Such multiband model effectively describes materials with caged structure [78] and shares many similarities with the dilute Kondo lattice, which is important for understanding the crossover between the Kondo impurity limit and the dense Kondo lattice limit. For the multiband case, one introduces a "band" index $\eta = 1, \dots, M$ to describe the conduction electrons, so that the Hamiltonian reads

$$H = \sum_{\mathbf{k}\alpha} \Psi^\dagger_{\mathbf{k}\alpha} T_{\mathbf{k}} \Psi_{\mathbf{k}\alpha} + \sum_{\mathbf{k}\eta\alpha\beta} \frac{J_K(\eta)}{2} c^\dagger_{\mathbf{k}\eta\alpha} \boldsymbol{\sigma}_{\alpha\beta} c_{\mathbf{k}\eta\beta} \cdot \boldsymbol{S}_{\mathbf{k}}, \quad (9)$$

where $\Psi_{\mathbf{k}\alpha} = (c_{\mathbf{k}1\alpha}, \dots, c_{\mathbf{k}M\alpha})^{\mathsf{T}}$, and $T_{\mathbf{k}}$ is an $M \times M$ kinetic energy matrix. This model can be exactly diagonalized as long as M is not too large.

In conclusion, our work shows that the $\mathbf{k}$-space Kondo/Anderson lattice model has the advantage over conventional real-space models in that it can be solved exactly, while at the same time it captures many important features of heavy-fermion materials, and thus it opens a new window toward the ultimate solving of heavy-fermion problems.

ACKNOWLEDGMENTS

The authors thank Y. Zhong and J. Herzog-Arbeitman for stimulating discussions. J.W. is supported by the Young Scientists Fund of the National Natural Science Foundation of China (Grant No. 12304174). Y.L. is supported by the Fundamental Research Funds for the Central Universities (Grant No. E2E44305). Y.-F.Y. is supported by the National Natural Science Foundation of China (Grants No. 12174429 and No. 11974397), the National Key Research and Development Program of China (Grant No. 2022YFA1402203), and the Strategic Priority Research Program of the Chinese Academy of Sciences (Grant No. XDB33010100).

APPENDIX A: DERIVATION OF THE k-SPACE KONDO MODEL

In this section, we derive the $\mathbf{k}$-space Kondo model from the Hatsugai-Kohmoto-Anderson lattice model [52]:

$$\begin{aligned} H &= H_c + H_f + H_{\text{hyb}}, \\ H_c &= \sum_{\mathbf{k}\alpha} \epsilon_{\mathbf{k}} c^\dagger_{\mathbf{k}\alpha} c_{\mathbf{k}\alpha}, \\ H_f &= \sum_{\mathbf{k}} \xi_{\mathbf{k}} n^f_{\mathbf{k}} + U \sum_{\mathbf{k}} n^f_{\mathbf{k}\uparrow} n^f_{\mathbf{k}\downarrow}, \\ H_{\text{hyb}} &= \mathcal{V} \sum_{\mathbf{k}\alpha} (c^\dagger_{\mathbf{k}\alpha} f_{\mathbf{k}\alpha} + \text{H.c.}). \end{aligned} \quad (A1)$$

Here $\xi_{\mathbf{k}} = \epsilon^f_{\mathbf{k}} - \mu_f$, $\epsilon^f_{\mathbf{k}} \in [-D_f, D_f]$ is the f-electron dispersion, and μ_f is its chemical potential. At $\mathcal{V} = 0$, the ground state of H_f is known exactly [46]. At half filling ($\mu_f = U/2$), the ground state is a NFL metal for $U < 2D_f$ and a Mott insulator for $U > 2D_f$. To describe heavy-fermion systems, here we assume half filling and $U \gg 2D_f$.

The $\mathbf{k}$-space Kondo model can be derived from a Schrieffer-Wolf (SW) transformation of the above model. We start with the low-energy states of $H_c + H_f$:

$$|l\rangle : \quad |\Psi\rangle_c \otimes \prod_{\mathbf{k}} |n^f_{\mathbf{k}} = 1\rangle, \quad (A2)$$

where $|\Psi\rangle_c$ denotes the eigenstates of H_c. Turning on the hybridization $\mathcal{V}$ will induce charge fluctuations and lead to high-energy states with $n^f_{\mathbf{q}} \neq 1$ at some momentum $\mathbf{q}$:

$$\begin{aligned}|h\rangle:\ & c_{\mathbf{q}\sigma}|\Psi\rangle_c \otimes f^\dagger_{\mathbf{q}\sigma}\prod_{\mathbf{k}}\big|n^f_{\mathbf{k}}=1\big\rangle,\\ & c^\dagger_{\mathbf{q}\sigma}|\Psi\rangle_c \otimes f_{\mathbf{q}\sigma}\prod_{\mathbf{k}}\big|n^f_{\mathbf{k}}=1\big\rangle.\end{aligned} \tag{A3}$$

Here we have ignored high-energy states with more than one empty or doubly occupied momentum point, which only give higher-order $[O(\mathcal{V}^4)]$ corrections. Using Eqs. (A2) and (A3) as a basis, one can rewrite Eq. (A1) into the following matrix form separating the low (L) and high energy (H) subspaces:

$$H = \begin{bmatrix} H_{\rm L} & M^\dagger \\ M & H_{\rm H}\end{bmatrix}, \tag{A4}$$

where $(H_{\rm L})_{ll'} = \langle l|H_c + H_f|l'\rangle$, $(H_{\rm H})_{hh'} = \langle h|H_c + H_f|h'\rangle$, and $M_{hl} = \langle h|H_{\rm hyb}|l\rangle$ mixes different subspaces. The SW transformation is a canonical transformation $\mathcal{U} = e^S$ that turns Eq. (A4) into block-diagonal form:

$$\mathcal{U}\begin{bmatrix} H_{\rm L} & M^\dagger \\ M & H_{\rm H}\end{bmatrix}\mathcal{U}^\dagger = \begin{bmatrix} H^* & 0 \\ 0 & H'\end{bmatrix}. \tag{A5}$$

Then $H_{\rm eff} = P_{\rm L}H^*P_{\rm L}$ provides the effective low-energy Hamiltonian, where $P_{\rm L} = \sum_l |l\rangle\langle l|$ is the projection operator. Equation (A5) is satisfied up to order $O(\mathcal{V}^2)$ if

$$S = \begin{bmatrix} 0 & -s^\dagger \\ s & 0\end{bmatrix}, \quad s_{hl} = \frac{M_{hl}}{E^{\rm H}_h - E^{\rm L}_l}, \tag{A6}$$

where $E^{\rm H}_h$ and $E^{\rm L}_l$ are the eigenvalues of $H_{\rm H}$ and $H_{\rm L}$. Substituting Eq. (A6) into Eq. (A5) leads to $H^* = H_L + \Delta H$, with

$$\begin{aligned}(\Delta H)_{ll'} &= -\frac{1}{2}\sum_h M^\dagger_{lh}M_{hl'}\left(\frac{1}{E^{\rm H}_h - E^{\rm L}_l} + \frac{1}{E^{\rm H}_h - E^{\rm L}_{l'}}\right)\\ &= \Delta H^{f^1+e^-\leftrightarrow f^2}_{ll'} + \Delta H^{f^1\leftrightarrow f^0+e^-}_{ll'},\end{aligned} \tag{A7}$$

where the last line corresponds to two different types of charge fluctuations in Eq. (A3). Using

$$E^{\rm H}_h - E^{\rm L}_l = \begin{cases}\xi_{\mathbf{k}} + U - \epsilon_{\mathbf{k}}, & f^1 + e^- \leftrightarrow f^2,\\ -\xi_{\mathbf{k}} + \epsilon_{\mathbf{k}}, & f^1 \leftrightarrow f^0 + e^-,\end{cases} \tag{A8}$$

one has

$$H^{f^1+e^-\leftrightarrow f^2}_{ll'} = -\mathcal{V}^2\sum_{\mathbf{k}\alpha\beta}\frac{\langle l|c^\dagger_{\mathbf{k}\alpha}f_{\mathbf{k}\alpha}f^\dagger_{\mathbf{k}\beta}c_{\mathbf{k}\beta}|l'\rangle}{\xi_{\mathbf{k}} + U - \epsilon_{\mathbf{k}}} \tag{A9}$$

and

$$H^{f^1\leftrightarrow f^0+e^-}_{ll'} = -\mathcal{V}^2\sum_{\mathbf{k}\alpha\beta}\frac{\langle l|f^\dagger_{\mathbf{k}\beta}c_{\mathbf{k}\beta}c^\dagger_{\mathbf{k}\alpha}f_{\mathbf{k}\alpha}|l'\rangle}{-\xi_{\mathbf{k}} + \epsilon_{\mathbf{k}}}. \tag{A10}$$

One important observation from Eqs. (A9) and (A10) is that the $\mathbf{k}$ point must be singly occupied by conduction electrons in both $|l\rangle$ and $|l'\rangle$ in order to give a nonzero matrix element for $\alpha \neq \beta$, which then leads to the Kondo spin-flip scattering. Therefore, the $\mathbf{k}$-space Kondo interaction only operates in the singly occupied (Ω_1) region, as is indeed revealed by the exact solution of H_K. After rearranging the four fermion operators in Eqs. (A9) and (A10), we obtain

$$P_{\rm L}\Delta H P_{\rm L} = \sum_{\mathbf{k}} J_K(\mathbf{k})\mathbf{s}_{\mathbf{k}}\cdot\mathbf{S}_{\mathbf{k}}, \tag{A11}$$

with a generally $\mathbf{k}$-dependent Kondo coupling,

$$\begin{aligned}J_K(\mathbf{k}) &= 2\mathcal{V}^2\left(\frac{1}{\xi_{\mathbf{k}} + U - \epsilon_{\mathbf{k}}} + \frac{1}{-\xi_{\mathbf{k}} + \epsilon_{\mathbf{k}}}\right)\\ &= \frac{8\mathcal{V}^2U}{U^2 - 4\epsilon^2_{\mathbf{k}}},\end{aligned} \tag{A12}$$

where we have assumed $\xi_{\mathbf{k}} = -U/2$ for the f electrons in the second line. For $U \gg D$, Eq. (A12) reduces to the constant Kondo coupling $J_K = 8\mathcal{V}^2/U$. Since $P_{\rm L}H_{\rm L}P_{\rm L} = H_c +$ constant, we finally obtain the $\mathbf{k}$-space Kondo model H_K studied in this paper.

APPENDIX B: QUASIPARTICLE DISPERSIONS

The quasiparticle dispersions can be calculated from the zero-temperature Green's function of conduction electrons, defined as $G(\mathbf{k}, t) = -i\theta(t)\langle\{c_{\mathbf{k}\sigma}(t), c^\dagger_{\mathbf{k}\sigma}\}\rangle$. The result is [58]

$$G(\mathbf{k},\omega) = \begin{cases}\frac{1/4}{\omega-\epsilon_{\mathbf{k}}+\frac{3J_K}{4}} + \frac{3/4}{\omega-\epsilon_{\mathbf{k}}-\frac{J_K}{4}}, & \mathbf{k}\in\Omega_0,\\ \frac{1/2}{\omega-\epsilon_{\mathbf{k}}-\frac{3J_K}{4}} + \frac{1/2}{\omega-\epsilon_{\mathbf{k}}+\frac{3J_K}{4}}, & \mathbf{k}\in\Omega_1,\\ \frac{1/4}{\omega-\epsilon_{\mathbf{k}}-\frac{3J_K}{4}} + \frac{3/4}{\omega-\epsilon_{\mathbf{k}}+\frac{J_K}{4}}, & \mathbf{k}\in\Omega_2.\end{cases} \tag{B1}$$

The poles of $G(\mathbf{k},\omega)$ give rise to two branches of quasiparticle dispersions intersecting with the Fermi level at FS_1 and FS_2 (there are another two branches located far away from the Fermi level):

$$\omega_\pm(\mathbf{k}) = \epsilon_{\mathbf{k}} \pm \frac{3J_K}{4}. \tag{B2}$$

The above equation is reminiscent of the mean-field c-f hybridized dispersions of the Kondo lattice model; both split the bare conduction dispersion into two branches. Here, the direct gap between the upper and lower branches is proportional to the Kondo coupling. For constant J_K, they have the same curvature as the bare conduction dispersion, hence no mass enhancement. However, if one uses the general $\mathbf{k}$-dependent Kondo coupling, Eq. (A12), then the direct gap $12\mathcal{V}^2U/(U^2 - 4\epsilon^2_{\mathbf{k}})$ reaches its minimum at the original Fermi surface $\epsilon_{\mathbf{k}} = 0$ and becomes larger away from it. This leads to the band bending and mass enhancement as shown in Fig. 5. Nevertheless, we noticed that the mass enhancement in this model is usually quite weak, and some fine-tuning is required to obtain an almost flat band near the Fermi energy. Therefore, we believe the usual local Kondo term is still needed to fully capture the "heavy fermion" property of real materials.

APPENDIX C: COOPER INSTABILITY

To study the pair-binding energy of conduction electrons, we consider the following variational wave function:

$$|\psi\rangle = \sum_{\mathbf{k}\in\Omega_0}\alpha_{\mathbf{k}}b^\dagger_{\mathbf{k}}|G\rangle + \sum_{\mathbf{k}\in\Omega_1}\beta_{\mathbf{k}}b^\dagger_{\mathbf{k}}|G\rangle, \tag{C1}$$

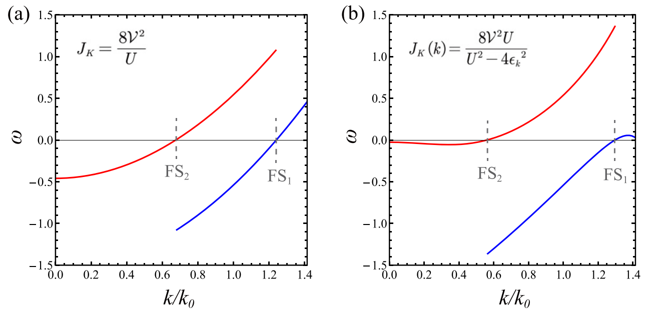

FIG. 5. Exact quasiparticle dispersions obtained from Eq. (B1) using (a) constant J_K and (b) momentum-dependent J_K for $\mathcal{V} = 0.52$ and $U = 3$.

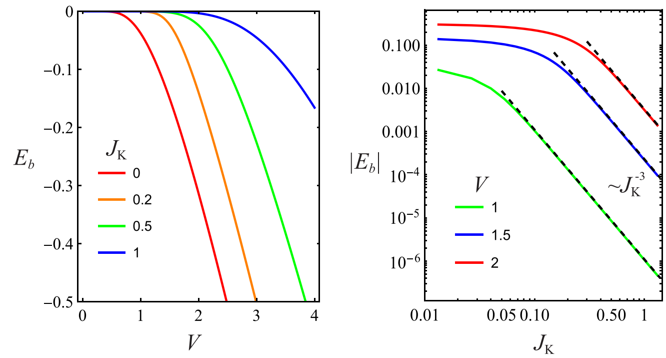

FIG. 6. The Cooper pair binding energy E_b as a function of V (left panel) and J_K (right panel). The dashed lines show J_K^{-3} dependence of $|E_b|$ at large J_K.

where $b_{\mathbf{k}}^{\dagger} = c_{\mathbf{k}\uparrow}^{\dagger} c_{-\mathbf{k}\downarrow}^{\dagger}$ creates a Cooper pair, $\alpha_{\mathbf{k}}$ and $\beta_{\mathbf{k}}$ are two variational parameters, and

$$|G\rangle = \prod_{\mathbf{k}} |g\rangle_{\mathbf{k}}, \tag{C2}$$

with

$$|g\rangle_{\mathbf{k}} = \begin{cases} \frac{1}{\sqrt{2}}(|0 \Uparrow\rangle + |0 \Downarrow\rangle), & \mathbf{k} \in \Omega_0, \\ \frac{1}{\sqrt{2}}(| \uparrow\Downarrow\rangle - | \downarrow\Uparrow\rangle), & \mathbf{k} \in \Omega_1, \\ \frac{1}{\sqrt{2}}(|2 \Downarrow\rangle + |2 \Uparrow\rangle), & \mathbf{k} \in \Omega_2, \end{cases} \tag{C3}$$

is the ground state of H_K. Here $|\phi\sigma\rangle$ denotes the conduction electron state $\phi = 0, \uparrow, \downarrow, 2$ and the f-spin state $\sigma = \Uparrow, \Downarrow$ at each momentum point. Note that each f spin in Ω_0 and Ω_2 has a twofold spin degeneracy, while here we choose the unpolarized state to calculate the binding energy [51]. The normalization condition of $|\psi\rangle$ gives the constraint

$$1 = \langle\psi|\psi\rangle = \sum_{\mathbf{k}\in\Omega_0} |\alpha_{\mathbf{k}}|^2 + \frac{1}{4} \sum_{\mathbf{k}\in\Omega_1} |\beta_{\mathbf{k}}|^2. \tag{C4}$$

The binding energy is defined as

$$E_b = \langle\psi|H'|\psi\rangle - \langle G|H'|G\rangle, \tag{C5}$$

where $H' = H_K + H_V$ is the total Hamiltonian including the pairing interaction

$$H_V = -\frac{V}{\mathcal{N}_s} \sum_{\mathbf{k}\mathbf{k}'} c_{\mathbf{k}\uparrow}^{\dagger} c_{-\mathbf{k}\downarrow}^{\dagger} c_{-\mathbf{k}'\downarrow} c_{\mathbf{k}'\uparrow}. \tag{C6}$$

The final result of E_b is

$$\begin{aligned} E_b = {} & 2 \sum_{\mathbf{k}\in\Omega_0} |\alpha_{\mathbf{k}}|^2 \epsilon_{\mathbf{k}} + \sum_{\mathbf{k}\in\Omega_1} \left(\frac{\epsilon_{\mathbf{k}}}{2} + \frac{3J_K}{8} \right) |\beta_{\mathbf{k}}|^2 \\ & - \frac{V}{\mathcal{N}_s} \sum_{\mathbf{k},\mathbf{k}'\in\Omega_0} \alpha_{\mathbf{k}'}^{*} \alpha_{\mathbf{k}} - \frac{V}{16\mathcal{N}_s} \sum_{\mathbf{k},\mathbf{k}'\in\Omega_1} \beta_{\mathbf{k}'}^{*} \beta_{\mathbf{k}} \\ & - \frac{V}{4\mathcal{N}_s} \sum_{\mathbf{k}\in\Omega_0,\mathbf{k}'\in\Omega_1} (\alpha_{\mathbf{k}} \beta_{\mathbf{k}'}^{*} + \alpha_{\mathbf{k}}^{*} \beta_{\mathbf{k}'}). \end{aligned} \tag{C7}$$

We then use the Lagrange multiplier method to find the minimum of E_b. By taking partial derivatives of the function $Q = E_b - \lambda(\langle\psi|\psi\rangle - 1)$ with respect to $\alpha_{\mathbf{k}}^{*}$ and $\beta_{\mathbf{k}}^{*}$, we have

$$\begin{aligned} 0 &= (2\epsilon_{\mathbf{k}} - \lambda)\alpha_{\mathbf{k}} - y, \\ 0 &= \left(2\epsilon_{\mathbf{k}} - \lambda + \frac{3J_K}{2}\right)\beta_{\mathbf{k}} - y, \end{aligned} \tag{C8}$$

where $y = \frac{V}{\mathcal{N}_s}(\sum_{\mathbf{k}\in\Omega_0} \alpha_{\mathbf{k}} + \frac{1}{4}\sum_{\mathbf{k}\in\Omega_1} \beta_{\mathbf{k}})$. Multiplying the above equations by $\alpha_{\mathbf{k}}^{*}$ and $\frac{1}{4}\beta_{\mathbf{k}}^{*}$, respectively, and summing over the momentum leads to $\lambda = E_b$. Thus we have

$$\begin{aligned} \alpha_{\mathbf{k}} &= \frac{y}{2\epsilon_{\mathbf{k}} - E_b}, \\ \beta_{\mathbf{k}} &= \frac{y}{2\epsilon_{\mathbf{k}} + \frac{3J_K}{2} - E_b}. \end{aligned} \tag{C9}$$

Substituting the above result into Eq. (C4) leads to

$$\begin{aligned} 1 = {} & \frac{1}{\mathcal{N}_s} \sum_{\mathbf{k}\in\Omega_0} \frac{V}{2\epsilon_{\mathbf{k}} - E_b} \\ & + \frac{1}{4\mathcal{N}_s} \sum_{\mathbf{k}\in\Omega_1} \frac{V}{2\epsilon_{\mathbf{k}} + \frac{3J_K}{2} - E_b}. \end{aligned} \tag{C10}$$

Using the density of states

$$\rho(\omega) = \frac{1}{\mathcal{N}_s} \sum_{\mathbf{k}} \delta(\omega - \epsilon_{\mathbf{k}}) = \frac{1}{2D}, \tag{C11}$$

we finally obtain

$$1 = \frac{V}{16D} \ln \left| \frac{(2D - E_b)^4 (3J_K - E_b)}{-(3J_K/2 - E_b)^4 E_b} \right|. \tag{C12}$$

For $J_K = 0$ and small V, the above equation reduces to the BCS result $E_b = -2De^{-4D/V}$. For $J_K, D \gg E_b$, we obtain the asymptotic behavior $E_b \propto -D^4 J_K^{-3} e^{-16D/V}$, as shown in Fig. 6.

APPENDIX D: FIRST-ORDER TRANSITIONS

Here we provide the full data of the temperature dependence of mean-field order parameter Δ_c at different J_K for $V = 1$, as shown in Fig. 7(a). The general behavior of Δ_c for $J_K \leqslant 0.3$ is similar to the BCS result at $J_K = 0$, except for the low-temperature minima at which Δ_F increases rapidly. For $J_K \geqslant 0.4$, Δ_c has a large slope at intermediate temperatures,

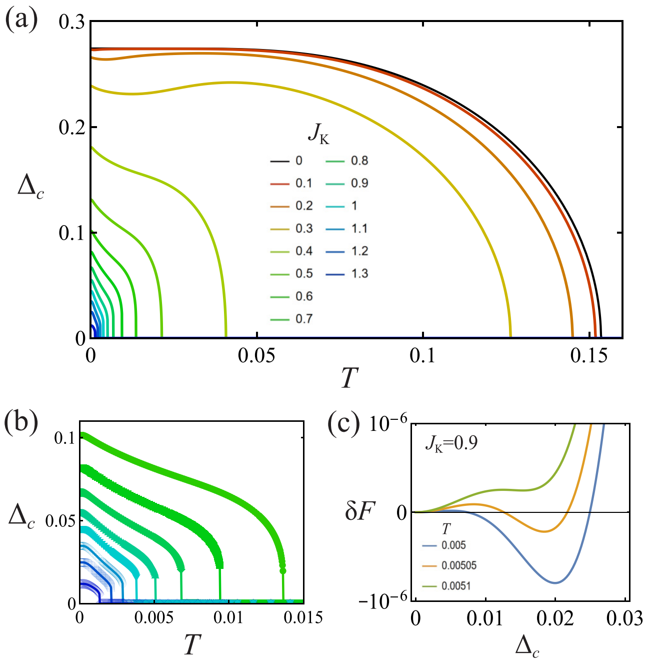

FIG. 7. (a) The mean-field order parameter Δ_c as a function of temperature at different J_K and $V = 1$. (b) An enlarged view of Δ_c for $0.6 \leqslant J_K \leqslant 1.3$, showing discontinuous jumps at T_c. (c) The free energy difference $\delta F = F(\Delta_c) - F(0)$ as a function of Δ_c around T_c for $J_K = 0.9$.

which is quite different from the BCS theory. For $J_K \geqslant 0.6$, Δ_c jumps discontinuously at T_c as shown in Fig. 7(b), indicating first-order transitions. Accordingly, the free energy as a function of Δ_c exhibits two minima at $\Delta_c = 0$ and $\Delta_c \neq 0$ within a small temperature window [see Fig. 7(c) for $J_K = 0.9$], corresponding to the metastable normal and superconducting states in the coexisting region of a weakly first-order transition.

APPENDIX E: COMPOSITE FERMION

The fact that the composite fermion corresponds to the SW transformation of the f electron has been noted earlier in Ref. [72]. Here we derive this result for the **k**-space Kondo model. We first notice that the f-electron annihilation (creation) operator itself connects the low-energy and high-energy subspaces, so it appears in the off-diagonal block of the matrix form in Eq. (A4). The canonical transformation $\mathcal{U} = e^S \approx 1 + S$ then transforms the f annihilation operator into

$$
e^S \begin{bmatrix} & f_{\mathbf{k}\sigma} \\ f_{\mathbf{k}\sigma} & \end{bmatrix} e^{-S} = \begin{bmatrix} -s^\dagger f_{\mathbf{k}\sigma} - f_{\mathbf{k}\sigma} s & f_{\mathbf{k}\sigma} \\ f_{\mathbf{k}\sigma} & s f_{\mathbf{k}\sigma} + f_{\mathbf{k}\sigma} s^\dagger \end{bmatrix} + O(\mathcal{V}^2). \tag{E1}
$$

Using the expression of s in Eq. (A6), we have the following renormalized f-electron operator in the low-energy subspace:

$$
\begin{aligned}
-P_\mathrm{L}(s^\dagger f_{\mathbf{k}\sigma} + f_{\mathbf{k}\sigma} s)P_\mathrm{L} &= -\sum_{ll'h} \frac{|l\rangle\langle l|\mathcal{V}\sum_{\mathbf{p}\alpha} c^\dagger_{\mathbf{p}\alpha} f_{\mathbf{p}\alpha} + \mathrm{H.c.}|h\rangle\langle h| f_{\mathbf{k}\sigma}|l'\rangle\langle l'|}{E^\mathrm{H}_h - E^\mathrm{L}_l} \\
&\quad - \sum_{ll'h} \frac{|l\rangle\langle l| f_{\mathbf{k}\sigma}|h\rangle\langle h|\mathcal{V}\sum_{\mathbf{p}\alpha} c^\dagger_{\mathbf{p}\alpha} f_{\mathbf{p}\alpha} + \mathrm{H.c.}|l'\rangle\langle l'|}{E^\mathrm{H}_h - E^\mathrm{L}_{l'}} \\
&\approx -\frac{2\mathcal{V}}{U} P_\mathrm{L} \sum_\alpha (f^\dagger_{\mathbf{k}\alpha} c_{\mathbf{k}\alpha} f_{\mathbf{k}\sigma} + f_{\mathbf{k}\sigma} f^\dagger_{\mathbf{k}\alpha} c_{\mathbf{k}\alpha}) P_\mathrm{L} \\
&= \frac{4\mathcal{V}}{U} F_{\mathbf{k}\sigma},
\end{aligned} \tag{E2}
$$

where

$$
\begin{aligned}
F_{\mathbf{k}\sigma} &= -\frac{1}{2} P_\mathrm{L} \sum_\alpha (f^\dagger_{\mathbf{k}\alpha} c_{\mathbf{k}\alpha} f_{\mathbf{k}\sigma} + f_{\mathbf{k}\sigma} f^\dagger_{\mathbf{k}\alpha} c_{\mathbf{k}\alpha}) P_\mathrm{L} \\
&= P_\mathrm{L}\left(f^\dagger_{\mathbf{k},-\sigma} f_{\mathbf{k}\sigma} c_{\mathbf{k},-\sigma} + f^\dagger_{\mathbf{k}\sigma} f_{\mathbf{k}\sigma} c_{\mathbf{k}\sigma} - \frac{1}{2} c_{\mathbf{k}\sigma} \right) P_\mathrm{L} \\
&= S^{-\sigma}_\mathbf{k} c_{\mathbf{k},-\sigma} + \frac{1}{2}(f^\dagger_{\mathbf{k}\sigma} f_{\mathbf{k}\sigma} - f^\dagger_{\mathbf{k},-\sigma} f_{\mathbf{k},-\sigma}) c_{\mathbf{k}\sigma} \\
&= S^{-\sigma}_\mathbf{k} c_{\mathbf{k},-\sigma} + \mathrm{sgn}(\sigma) S^z_\mathbf{k} c_{\mathbf{k}\sigma} \\
&= \sum_\beta \boldsymbol{\sigma}_{\sigma\beta} \cdot \mathbf{S}_\mathbf{k} c_{\mathbf{k}\beta}
\end{aligned} \tag{E3}
$$

is just the composite fermion operator defined in Eq. (8).

[1] C. Pfleiderer, Superconducting phases of f-electron compounds, Rev. Mod. Phys. **81**, 1551 (2009).
[2] B. D. White, J. D. Thompson, and M. B. Maple, Unconventional superconductivity in heavy-fermion compounds, Physica C (Amsterdam, Neth.) **514**, 246 (2015).
[3] F. Steglich and S. Wirth, Foundations of heavy-fermion superconductivity: Lattice Kondo effect and Mott physics, Rep. Prog. Phys. **79**, 084502 (2016).
[4] N. D. Mathur, F. M. Grosche, S. R. Julian, I. R. Walker, D. M. Freye, R. K. W. Haselwimmer, and G. G. Lonzarich, Magnetically mediated superconductivity in heavy fermion compounds, Nature (London) **394**, 39 (1998).
[5] C. Petrovic, P. G. Pagliuso, M. F. Hundley, R. Movshovich, J. L. Sarrao, J. D. Thompson, Z. Fisk, and P. Monthoux, Heavy-fermion superconductivity in $CeCoIn_5$ at 2.3 K, J. Phys.: Condens. Matter **13**, L337 (2001).
[6] H. Q. Yuan, F. M. Grosche, M. Deppe, C. Geibel, G. Sparn, and F. Steglich, Observation of two distinct superconducting phases in $CeCu_2Si_2$, Science **302**, 2104 (2003).
[7] T. Park, F. Ronning, H. Q. Yuan, M. B. Salamon, R. Movshovich, J. L. Sarrao, and J. D. Thompson, Hidden magnetism and quantum criticality in the heavy fermion superconductor $CeRhIn_5$, Nature (London) **440**, 65 (2006).
[8] E. Schuberth, M. Tippmann, L. Steinke, S. Lausberg, A. Steppke, M. Brando, C. Krellner, C. Geibel, R. Yu, Q. Si, and F. Steglich, Emergence of superconductivity in the canonical heavy-electron metal $YbRh_2Si_2$, Science **351**, 485 (2016).

[9] D. Aoki, K. Ishida, and J. Flouquet, Review of U-based ferromagnetic superconductors: Comparison between UGe_2, URhGe, and UCoGe, J. Phys. Soc. Jpn. **88**, 022001 (2019).
[10] S. Ran, C. Eckberg, Q.-P. Ding, Y. Furukawa, T. Metz, S. R. Saha, I.-L. Liu, M. Zic, H. Kim, J. Paglione, and N. P. Butch, Nearly ferromagnetic spin-triplet superconductivity, Science **365**, 684 (2019).
[11] A. T. Holmes and D. Jaccard, Signatures of valence fluctuations in $CeCu_2Si_2$ under high pressure, Phys. Rev. B **69**, 024508 (2004).
[12] B. J. Ramshaw, A. Shekhter, R. D. McDonald, J. B. Betts, J. N. Mitchell, P. H. Tobash, C. H. Mielke, E. D. Bauer, and A. Migliori, Avoided valence transition in a plutonium, Proc. Natl. Acad. Sci. USA **112**, 3285 (2015).
[13] S. Nakatsuji, D. Pines, and Z. Fisk, Two fluid description of the Kondo lattice, Phys. Rev. Lett. **92**, 016401 (2004).
[14] N. J. Curro, B.-L. Young, J. Schmalian, and D. Pines, Scaling in the emergent behavior of heavy-electron materials, Phys. Rev. B **70**, 235117 (2004).
[15] Y.-F. Yang and D. Pines, Universal behavior in heavy-electron materials, Phys. Rev. Lett. **100**, 096404 (2008).
[16] Y.-F. Yang, Z. Fisk, H.-O. Lee, J. D. Thompson, and D. Pines, Scaling the Kondo lattice, Nature (London) **454**, 611 (2008).
[17] Y.-F. Yang and D. Pines, Emergent states in heavy-electron materials, Proc. Natl. Acad. Sci. USA **109**, E3060 (2012).
[18] Y.-F. Yang, Anomalous Hall effect in heavy electron materials, Phys. Rev. B **87**, 045102 (2013).
[19] Y.-F. Yang and D. Pines, Quantum critical behavior in heavy electron materials, Proc. Natl. Acad. Sci. USA **111**, 8398 (2014).
[20] Y.-F. Yang and D. Pines, Emergence of superconductivity in heavy-electron materials, Proc. Natl. Acad. Sci. USA **111**, 18178 (2014).
[21] Y.-F. Yang, Two-fluid model for heavy electron physics, Rep. Prog. Phys. **79**, 074501 (2016).
[22] G. Lonzarich, D. Pines, and Y.-F. Yang, Toward a new microscopic framework for Kondo lattice materials, Rep. Prog. Phys. **80**, 024501 (2017).
[23] Y.-F. Yang, D. Pines, and G. Lonzarich, Quantum critical scaling and fluctuations in Kondo lattice materials, Proc. Natl. Acad. Sci. USA **114**, 6250 (2017).
[24] J. D. Thompson and Z. Fisk, Progress in heavy-fermion superconductivity: Ce115 and related materials, J. Phys. Soc. Jpn. **81**, 011002 (2012).
[25] G. R. Stewart, Unconventional superconductivity, Adv. Phys. **66**, 75 (2017).
[26] Y. Kohori, Y. Yamato, Y. Iwamoto, T. Kohara, E. D. Bauer, M. P. Maple, and J. L. Sarrao, NMR and NQR studies of the heavy fermion superconductors $CeTIn_5$ ($T = $ Co and Ir), Phys. Rev. B **64**, 134526 (2001).
[27] T. Mito, S. Kawasaki, G.-q. Zheng, Y. Kawasaki, K. Ishida, Y. Kitaoka, D. Aoki, Y. Haga, and Y. Onuki, Pressure-induced anomalous magnetism and unconventional superconductivity in $CeRhIn_5$: ^{115}In-NQR study under pressure, Phys. Rev. B **63**, 220507(R) (2001).
[28] G.-q. Zheng, K. Tanabe, T. Mito, S. Kawasaki, Y. Kitaoka, D. Aoki, Y. Haga, and Y. Onuki, Unique spin dynamics and unconventional superconductivity in the layered heavy fermion compound $CeIrIn_5$: NQR evidence, Phys. Rev. Lett. **86**, 4664 (2001).
[29] Y. Mizukami, H. Shishido, T. Shibauchi, M. Shimozawa, S. Yasumoto, D. Watanabe, M. Yamashita, H. Ikeda, T. Terashima, H. Kontani, and Y. Matsuda, Extremely strong-coupling superconductivity in artificial two-dimensional Kondo lattices, Nat. Phys. **7**, 849 (2011).
[30] D. Daghero, M. Tortello, G. A. Ummarino, J.-C. Griveau, E. Colineau, R. Eloirdi, A. B. Shick, J. Kolorenc, A. I. Lichtenstein, and R. Caciuffo, Strong-coupling d-wave superconductivity in $PuCoGa_5$ probed by point-contact spectroscopy, Nat. Commun. **3**, 786 (2012).
[31] S. Nishiyama, K. Miyake, and C. M. Varma, Superconducting transition temperatures for spin-fluctuation superconductivity: Application to heavy-fermion compounds, Phys. Rev. B **88**, 014510 (2013).
[32] Y. Li, M. Liu, Z. Fu, X. Chen, F. Yang, and Y.-F. Yang, Gap symmetry of the heavy fermion superconductor $CeCu_2Si_2$ at ambient pressure, Phys. Rev. Lett. **120**, 217001 (2018).
[33] J. C. Xavier and E. Dagotto, Robust d-wave pairing correlations in the Heisenberg Kondo lattice model, Phys. Rev. Lett. **100**, 146403 (2008).
[34] R. Flint and P. Coleman, Tandem pairing in heavy-fermion superconductors, Phys. Rev. Lett. **105**, 246404 (2010).
[35] Y. Liu, H. Li, G.-M. Zhang, and L. Yu, d-wave superconductivity induced by short-ranged antiferromagnetic correlations in the two-dimensional Kondo lattice model, Phys. Rev. B **86**, 024526 (2012).
[36] W. Wu and A.-M.-S. Tremblay, d-wave superconductivity in the frustrated two-dimensional periodic Anderson model, Phys. Rev. X **5**, 011019 (2015).
[37] H. Hu, A. Cai, L. Chen, L. Deng, J. H. Pixley, K. Ingersent, and Q. Si, Unconventional superconductivity from Fermi surface fluctuations in strongly correlated metals, arXiv:2109.13224.
[38] V. Barzykin, Two-fluid behavior of the Kondo liquid in the $1/N$ slave boson approach, Phys. Rev. B **73**, 094455 (2006).
[39] M. Jiang, N. J. Curro, and R. T. Scalettar, Universal Knight shift anomaly in the periodic Anderson model, Phys. Rev. B **90**, 241109(R) (2014).
[40] N. Xie and Y.-F. Yang, Interplay of localized and itinerant behavior in the one-dimensional Kondo-Heisenberg model, Phys. Rev. B **91**, 195116 (2015).
[41] Y.-F. Yang, N. Xie, and Y. Li, Two-fluid theory for heavy fermion materials, Prog. Phys. **35**, 191 (2015).
[42] M. Jiang and Y.-F. Yang, Universal scaling in the Knight-shift anomaly of the doped periodic Anderson model, Phys. Rev. B **95**, 235160 (2017).
[43] J.-J. Dong, D. Huang, and Y.-F. Yang, Mutual information, quantum phase transition, and phase coherence in Kondo systems, Phys. Rev. B **104**, L081115 (2021).
[44] J.-J. Dong and Y.-F. Yang, Development of long-range phase coherence on the Kondo lattice, Phys. Rev. B **106**, L161114 (2022).
[45] Y. Hatsugai and M. Kohmoto, Exactly solvable model of correlated lattice electrons in any dimensions, J. Phys. Soc. Jpn. **61**, 2056 (1992).
[46] P. W. Phillips, L. Yeo, and E. W. Huang, Exact theory for superconductivity in a doped Mott insulator, Nat. Phys. **16**, 1175 (2020).
[47] E. W. Huang, G. L. Nava, and P. W. Phillips, Discrete symmetry breaking defines the Mott quartic fixed point, Nat. Phys. **18**, 511 (2022).

[48] J. Zhao, G. L. Nave, and P. W. Phillips, Proof of a stable fixed point for strongly correlated electron matter, Phys. Rev. B **108**, 165135 (2023).

[49] K. Yang, Exactly solvable model of Fermi arcs and pseudogap, Phys. Rev. B **103**, 024529 (2021).

[50] C. Setty, Superconductivity from Luttinger surfaces: Emergent Sachdev-Ye-Kitaev physics with infinite-body interactions, Phys. Rev. B **103**, 014501 (2021).

[51] Y. Li, V. Mishra, Y. Zhou, and F.-C. Zhang, Two-stage superconductivity in the Hatsugai-Kohomoto-BCS model, New J. Phys. **24**, 103019 (2022).

[52] Y. Zhong, Solvable periodic Anderson model with infinite-range Hatsugai-Kohmoto interaction: Ground-states and beyond, Phys. Rev. B **106**, 155119 (2022).

[53] M. Zhao, W.-W. Yang, H.-G. Luo, and Y. Zhong, Friedel oscillation in non-Fermi liquid: Lesson from exactly solvable Hatsugai-Kohmoto model, J. Phys.: Condens. Matter **35**, 495603 (2023).

[54] W.-W. Yang, H.-G. Luo, and Y. Zhong, Bose metal in an exactly solvable model with infinite-range Hatsugai-Kohmoto interaction, Phys. Rev. B **108**, 235149 (2023).

[55] P. Mai, J. Zhao, B. E. Feldman, and P. W. Phillips, 1/4 is the new 1/2 when topology is intertwined with Mottness, Nat. Commun. **14**, 5999 (2023).

[56] P. Mai, B. E. Feldman, and P. W. Phillips, Topological Mott insulator at quarter filling in the interacting Haldane model, Phys. Rev. Res. **5**, 013162 (2023).

[57] K. Jabłonowski, J. Skolimowski, W. Brzezicki, K. Byczuk, and M. M. Wysoiński, Topological Mott insulator in the odd-integer filled Anderson lattice model with Hatsugai-Kohmoto interactions, Phys. Rev. B **108**, 195145 (2023).

[58] J. Wang and Y.-F. Yang, Nonlocal Kondo effect and two-fluid picture revealed in an exactly solvable model, PNAS Nexus **2**, pgad169 (2023).

[59] D. Chowdhury, A. Georges, O. Parcollet, and S. Sachdev, Sachdev-Ye-Kitaev models and beyond: Window into non-Fermi liquids, Rev. Mod. Phys. **94**, 035004 (2022).

[60] G. Baskaran, An exactly solvable fermion model: Spinons, holons and a non-Fermi liquid phase, Mod. Phys. Lett. B **05**, 643 (1991).

[61] T.-K. Ng, Beyond Fermi-liquid theory: The k-Fermi liquids, arXiv:1910.06602.

[62] J. Wang and Y.-F. Yang, Nonlocal Kondo effect and quantum critical phase in heavy-fermion metals, Phys. Rev. B **104**, 165120 (2021).

[63] J. Wang and Y.-F. Yang, Z_2 metallic spin liquid on a frustrated Kondo lattice, Phys. Rev. B **106**, 115135 (2022).

[64] J. Wang and Y.-F. Yang, Spin current Kondo effect in frustrated Kondo systems, Sci. China Phys. Mech. Astron. **65**, 227212 (2022).

[65] J. Chen, J. Wang, and Y.-F. Yang, Pair density wave, unconventional superconductivity, and non-Fermi liquid quantum critical phase in frustrated Kondo lattice, Phys. Rev. B **109**, 014103 (2024).

[66] A. A. Patel, M. J. Lawler, and E.-A. Kim, Coherent superconductivity with a large gap ratio from incoherent metals, Phys. Rev. Lett. **121**, 187001 (2018).

[67] Y. Zhou, J. Guo, S. Cai, J. Zhao, G. Gu, C. Lin, H. Yan, C. Huang, C. Yang, S. Long, Y. Gong, Y. Li, X. Li, Q. Wu, J. Hu, X. Zhou, T. Xiang, and L. Sun, Quantum phase transition from superconducting to insulating-like state in a pressurized cuprate superconductor, Nat. Phys. **18**, 406 (2022).

[68] J. Han, X. Zhu, J. Zhang, S. Cai, J. Guo, Y. Zhou, J. Zhao, P. Wang, L. Wang, X. Wei, S. Jiang, K. Yang, Y. Gong, Y. Li, X. Li, L. Cao, M. Tian, Q. Wu, T. Xiang, and L. Sun, Superconducting-insulating quantum phase transition associated with valence change in compressed perovskite bismuth-oxides, arXiv:2305.08406.

[69] T.-H. Lee, A. Chubukov, H. Miao, and G. Kotliar, Pairing mechanism in Hund's metal superconductors and the universality of the superconducting gap to critical temperature ratio, Phys. Rev. Lett. **121**, 187003 (2018).

[70] Y.-M. Wu, A. Abanov, and A. V. Chubukov, Pairing in quantum critical systems: Transition temperature, pairing gap, and their ratio, Phys. Rev. B **99**, 014502 (2019).

[71] M. Maltseva, M. Dzero, and P. Coleman, Electron cotunneling into a Kondo lattice, Phys. Rev. Lett. **103**, 206402 (2009).

[72] B. Danu, Z. Liu, F. F. Assaad, and M. Raczkowski, Zooming in on heavy fermions in Kondo lattice models, Phys. Rev. B **104**, 155128 (2021).

[73] J. Chen, E. M. Stoudenmire, Y. Komijani, and P. Coleman, Matrix product study of spin fractionalization in the 1D Kondo insulator, arXiv:2302.09701.

[74] S. Ikeda, H. Shishido, M. Nakashima, R. Settai, D. Aoki, Y. Haga, H. Harima, Y. Aoki, T. Namiki, H. Sato, and Y. Onuki, Unconventional superconductivity in $CeCoIn_5$ studied by the specific heat and magnetization measurements, J. Phys. Soc. Jpn. **70**, 2248 (2001).

[75] W. K. Park, J. L. Sarrao, J. D. Thompson, and L. H. Greene, Andreev reflection in heavy-fermion superconductors and order parameter symmetry in $CeCoIn_5$, Phys. Rev. Lett. **100**, 177001 (2008).

[76] T. Park and J. D. Thompson, Magnetism and superconductivity in strongly correlated $CeRhIn_5$, New J. Phys. **11**, 055062 (2009).

[77] V. Barzykin and L. P. Gor'kov, Competition between phonon superconductivity and Kondo screening in mixed valence and heavy fermion compounds, Phys. Rev. B **71**, 214521 (2005).

[78] C. L. Yang, X. Wang, X. Zhang, D. S. Wu, M. Liu, P. Zheng, J. Y. Yao, Z. Z. Li, Y.-F. Yang, Y. G. Shi, J. L. Luo, and N. L. Wang, Kondo effect in the quasiskutterudite $Yb_3Os_4Ge_{13}$, Phys. Rev. B **91**, 075120 (2015).